Journal of Zhejiang University SCIENCE A
ISSN 1673-565X (Print); ISSN 1862-1775 (Online)
www.zju.edu.cn/jzus; www.springerlink.com
E-mail: jzus@zju.edu.cn

Simulated moving bed separation of tocopherol homologues: simulation and experiments*

Yu-bin LÜ[†1,2], Bao-gen SU[†‡1], Yi-wen YANG[1], Qi-long REN[1], Ping-dong WU[1]

([1]*National Laboratory of Secondary Resources Chemical Engineering, Zhejiang University, Hangzhou 310027, China*)

([2]*Hangzhou Zhongmei Huadong Pharmaceutical Co., Ltd., Hangzhou 310011, China*)

[†]E-mail: lvyubin2001@zju.edu.cn; subg@zju.edu.cn

Received June 1, 2008; Revision accepted Nov. 11, 2008; Crosschecked Feb. 25, 2009

Abstract: Chromatograms of tocopherol homologues were obtained by a column of analytical size (inner diameter (ID) 0.46 cm cm×10 cm) packed with silica gel. Adsorption isotherms and film mass-transfer coefficient were estimated from the chromatograms by using a general rate model, which considers axial dispersion, external mass-transfer and intraparticle diffusion. Based on the obtained isotherms and mass-transfer coefficient, the separation process of tocopherol homologues on simulated moving bed (SMB) was simulated using the same model. According to the simulated results, a mixture of α-, γ-, δ-tocopherols and other impurities was separated on an SMB equipment. The SMB equipment was composed of 8 columns of ID 2 cm×10 cm, with 2 columns in each section. The solid phase was silica gel, and the mobile phase was *n*-hexane/2-propanol (99/1 by volume). γ- and δ-tocopherols of purity greater than 98% were obtained with recovery greater than 98%. The effects of operating conditions (flow rates and switching time) on the performance of SMB were studied by both simulation and experiments. It was found that all the simulation results were quite close to the experimental results. We conclude that process development and optimization of operating conditions of SMB by simulation are feasible.

Key words: Simulated moving bed (SMB), Separation, Modeling, Simulation, Tocopherol homologues
doi:10.1631/jzus.A0850108 **Document code:** A **CLC number:** TQ028.3

INTRODUCTION

Tocopherols are natural products widely used as vitamin E for human health, cosmetics ingredient, and food antioxidant. The main resource of tocopherols is the deodorized distillate produced by the manufacture process of edible oil. The main constituents of the tocopherols extracted from deodorized distillate are α, β, γ, and δ-tocopherols. Their molecular structures have a common core ring, differing only in the number of attached methyl groups. Although the structures are quite similar, it is found that α-tocopherol has the highest biopotency among all the isomeric forms. Yang *et al.*(2004) reported transformation of tocopherols, other than α-tocopherol, to α-tocopherol; however, an efficient separation and purification process of tocopherols remains un-reported.

Simulated moving bed (SMB) is a continuous chromatographic countercurrent process and has been widely used in large scale in the past few decades (Schulte and Strube, 2001). Compared to preparative chromatography, both the adsorbent inventory and the solvent consumption in SMB are much less (Jupke *et al.*, 2002; Bruce, 1998). In addition, high performance can be achieved even when the selectivity of the adsorbent to the components to be separated is rather low. Fig.1 shows a standard four-section SMB unit (LÜ *et al.*, 2006). The system consists of four sections packed with a solid phase (adsorbent). The feed to be separated is introduced between sections 2 and 3. The component with lower affinity (the

‡ Corresponding author
* Project (No. 20040335045) supported by the Specialized Research Fund for the Doctoral Program of Higher Education of China

raffinate) to the solid phase is collected between sections 3 and 4, and that with higher affinity (the extract) is collected between sections 1 and 2. The desorbent is introduced between sections 4 and 1 to regenerate the solid phase. Part of the liquid phase is recycled to section 1 after being washed in section 4. In the SMB, the counter-current movement of the solid is achieved by periodic switching of the ports of inlet and outlet in the direction of the fluid flow. This can be done either by a rotary valve or through a set of individual valves switched at programmed times.

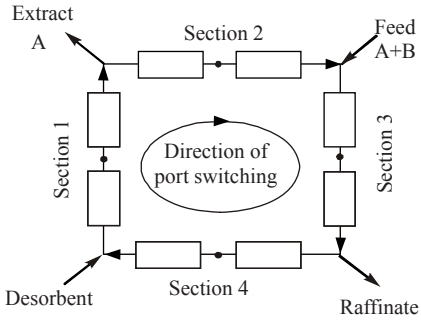

Fig.1 Scheme of a four-section SMB unit (Lü *et al*., 2006)

A key issue in developing an SMB process is the determination of operating conditions including flow rates in the four sections and the switching time. Many methods for SMB design have been reported, including the triangle theory method (Mazzotti *et al.*, 1997; Migliorini *et al.*, 1998), the standing wave method (Ma and Wang, 1997), the safety margin method (Ruthven and Ching, 1989; Zhong and Guiochon, 1998), and the rate model (Minceva and Rodrigues, 2002; Xie *et al.*, 2003; LÜ *et al*., 2006). The triangle theory based on equilibrium theory is applicable to ideal systems where mass-transfer effects are negligible. For most realistic systems, the significant mass-transfer effect must be taken into account by trial-and-error experiments to fine tune the operating conditions. Similarly, the safety margin method is also based on the equilibrium theory but provides an empirical margin to treat the mass-transfer effect. The rate model consists of a set of partial differential equations (PDEs) for unsteady-state multicomponent dispersion and film diffusion in the mobile phase and internal diffusion in the stationary phase as well. If the adsorption isotherms and mass-transfer parameters are accurate, simulation by the rate model can give reliable predictions of column profiles, effluent histories, and product purities and yields.

The present work intended to develop a process for separation of the tocopherol homologues by using SMB. We obtained the adsorption isotherms and film mass-transfer coefficient based on the experimental chromatograms obtained by a small size column, and then simulated the SMB process under different operating conditions using the general rate (G-R) model. Finally, we carried out separation experiments to verify the simulated results.

MODELING

There are two approaches for modeling an SMB process (Dunnebier and Klatt, 2000). One is the true moving-bed (TMB) model, which assumes an equivalent countercurrent movement of the solid phase, neglects the dynamics associated with periodic switching, and produces mean concentration profiles over a switching period. Theoretically, the TMB model describes the situation with infinite columns in each section. However, experience shows that this simplifying assumption still holds true in the case of relatively coarse subdivisions, for example, 2~4 columns in each section. The other approach used in this study is more rigorous, involving a representation of the system as an arrangement of static chromatography columns and taking periodic switching into account. This approach proved more accurate for simulation of the real process in the currrent study. The SMB modeling consists of two parts: the column and node models.

Column model

A rate model, which considers axial dispersion, external mass-transfer, intraparticle diffusion, and nonlinear isotherms, is considered to be a general multicomponent rate model (Gu *et al.*, 1995). Such a general model is adequate in most cases to describe the adsorption and mass-transfer processes in multicomponent chromatography. The following equations can be formulated from the differential mass balance for each component in the bulk-fluid and the particle phases.

$$-D_{bi}\frac{\partial^2 C_{bi}}{\partial Z^2}+u\frac{\partial C_{bi}}{\partial Z}+\frac{\partial C_{bi}}{\partial t}+\frac{3k_{fi}(1-\varepsilon_b)}{R_p\varepsilon_b}(C_{bi}-C_{pi,R=R_p})=0, \quad (1)$$

$$(1-\varepsilon_p)\frac{\partial C_{pi}^*}{\partial t}+\varepsilon_p\frac{\partial C_{pi}}{\partial t}-\varepsilon_p D_{pi}\left[\frac{1}{R^2}\frac{\partial}{\partial R}\left(R^2\frac{\partial C_{pi}}{\partial R}\right)\right]=0, \quad (2)$$

where C_{bi} is bulk-fluid phase concentration of component i, mg/ml; C_{pi} is concentration of component i in the stagnant fluid phase inside the particle macropores, mg/ml; C_{pi}^* is concentration of component i in the solid phase of the particle, mg/ml; D_{bi} is axial or radial dispersion coefficient of component i, cm^2/s; D_{pi} is effective diffusivity of component i, cm^2/s; k_{fi} is film mass-transfer coefficient of component i, cm/s; ε_b is bed void volume fraction; ε_p is particle porosity.

With the initial and boundary conditions:

$$t=0,\ C_{bi}=C_{bi}(0,Z),\ C_{pi}=C_{pi}(0,R,Z), \quad (3)$$

$$Z=0,\quad -\frac{\partial C_{bi}}{\partial Z}=\frac{u}{D_{bi}}(C_{bi}-C_{fi}(t)), \quad (4)$$

$$Z=L,\quad \frac{\partial C_{bi}}{\partial Z}=0, \quad (5)$$

$$R=0,\quad \frac{\partial C_{pi}}{\partial R}=0, \quad (6)$$

$$R=R_p,\quad \frac{\partial C_{pi}}{\partial R}=\frac{ki}{\varepsilon_p D_{pi}}(C_{bi}-C_{pi,R=R_p}), \quad (7)$$

Eqs.(1) and (2) are coupled via $C_{pi,R=R_p}$ which is the concentration of component i at the surface of a particle. In Eq.(2), C_{pi}^* is the concentration of component i in the solid phase (adsorbent) based on the unit volume of the solid, excluding pores. It is directly linked to the multicomponent isotherms, which couple the PDEs system. Concentrations C_{bi} and C_{pi} are based on the unit volume of mobile phase fluid. The effective diffusivities, D_{pi}, do not include the particle porosity.

Node model

The flow and integral mass balance equations at each node are given by Eqs.(8a)~(8d):

$$Q_4+Q_D=Q_1,\ C_{i,4}^{out}Q_4=C_{i,1}^{in}Q_1,\ \text{for desorbent node;} \quad (8a)$$

$$Q_1-Q_E=Q_2,\ C_{i,1}^{out}=C_{i,2}^{in},\ \text{for extract node;} \quad (8b)$$

$$Q_2+Q_F=Q_3,\ C_{i,2}^{out}Q_2+C_{i,F}Q_F=C_{i,3}^{in}Q_3,\ \text{for feed node;} \quad (8c)$$

$$Q_3-Q_R=Q_4,\ C_{i,3}^{out}=C_{i,4}^{in},\ \text{for raffinate node,} \quad (8d)$$

where $C_{i,j}^{out}$ and $C_{i,j}^{in}$ are the concentrations of component i at the outlet and the inlet of column j, respectively; Q_1, Q_2, Q_3, and Q_4 are the flow rates through the corresponding columns related to the liquid phase velocity by $Q_j=\varepsilon_b A u_j$, where A is the geometrical cross-sectional area; Q_D, Q_E, Q_F and Q_R are the flow rates of desorbent, extract, feed and raffinate, respectively. These equations are integral mass balances, which assume that there is no dispersion at these nodes.

Numerical solution of the model

An efficient and robust numerical procedure has been developed by Gu *et al*.(1995) for the solution of the above PDE system. It involves two steps. At the first step, the spatial axes, z and r, are discrete N_z axial elements and N_r collocation points. The bulk-fluid phase and the particle equations are separated by the finite element (FE) and the orthogonal collocation (OC) methods, respectively. Then the resulting $N_i(N_z)(N_r+1)$ ordinary differential equation (ODE) system (with initial values) is solved using an existing ODE solver provided by MATLAB®.

EXPERIMENTAL

Adsorption isotherm and film mass-transfer coefficient determination

An analytical column (inner diameter (ID) 0.46 cm×10 cm) was packed with the silica gel same as that used for SMB columns. The total porosity (ε_t) of the column was determined by the retention volume of a pulse of 1, 3, 5-tri-tert-butyl-benzene (assumed to be a non-retained species). The particle porosity of silica-gel (ε_p) was 0.45, and the bed voidage (ε_b) was 0.49, calculated by the following equation:

$$\varepsilon_b=\frac{\varepsilon_t-\varepsilon_p}{1-\varepsilon_p}.$$

The mobile phase was *n*-hexane/2-propanol

(99/1 by volume). Pulses of diluted tocopherol mixture were injected into the column to obtain the chromatograms. Based on these chromatograms the Henry constant of adsorption isotherm and the film mass-transfer coefficient were determined.

SMB experiments

The SMB unit was a CSEP 9116 from Knauer, Berlin. It consisted of a carousel of 8 stainless steel columns (ID 2 cm×10 cm) connected to a single multi-function valve. The column configuration of SMB was 2 columns in each section. There were 2 HPLC pumps (K-501, Knauer) pumping the feed and the desorbent, and another 2 pumps partially recycling the inner currents from sections 1 into 2 and from sections 3 into 4. The temperature of the columns was maintained at 30 °C by enclosing the entire rotating system within a thermostat.

The stationary phase was silica gel (length 20~30 μm, Brunauer-Enmet-Teller surface area 312 m^2/g, average pore diameter 11.8 nm) purchased from Meigao Chemical Group (Qingdao, China). The columns were packed with silica gel by the slurry-packing technique. For SMB, it is essential that the packing in each of the 8 columns has the same porosity. The total porosity of each column was determined by retention volume of 1,3,5-tri-tert-butyl-benzene (Table 1). The deviation of the maximum total porosity to the average value was within 3%. The mobile phase used in the 8 columns was *n*-hexane/2-propanol (99/1 by volume) with a flow rate of 5.0 ml/min.

Table 1 Determination of total porosity of the SMB columns

Column No.	Retention time of 1,3,5-tri-tert-butyl-benzene (min)	Total porosity (ε_t)	Bed voidage (ε_b)
1	4.464	0.711	0.47
2	4.413	0.703	0.46
3	4.498	0.716	0.48
4	4.448	0.708	0.47
5	4.540	0.723	0.50
6	4.565	0.727	0.50
7	4.332	0.690	0.44
8	4.432	0.706	0.47
Average	4.462	0.711	0.47

Before each SMB experiment, the flow rates of the four pumps were set manually and were checked later periodically during the experiment to ensure accuracy. The switching time was set by the SMB controller.

Samples were collected from the extract and raffinate ports continuously over an entire switching period (between two switches) and were analyzed. Therefore, the composition of each sample represented the average composition of the extract or the raffinate over a switching period. The SMB experiments were stopped at the point that the average composition was unchanged; i.e., the cyclic steady state was reached. Then samples were collected at a definite time from all the ports. The composition of these samples represented the instant composition of a definite position along the columns so that the composition profile at a definite time was obtained.

The composition of each sample was determined by HPLC. The HPLC column was of ID 0.46 cm×25 cm, packed with silica gel (5 μm in length). The mobile phase was *n*-hexane/2-propanol (99/1 by volume), at a flow rate of 1.0 ml/min. The UV detector was from Knauer, and the wavelength used was 292 nm. α-, γ- and δ-tocopherols purchased from Sigma (purity>95%; USA) were used as a standard for quantitative determination. The tocopherol concentrate (with 5.1% α-tocopherol, 43.82% γ-tocopherol and 48.13% δ-tocopherol) was purchased from Jiusan Lipids Company (Heilongjiang, China).

RESULTS AND DISCUSSIONS

Adsorption isotherms

Since the concentration of tocopherols in the feed of SMB was quite low (28 mg/ml), linear adsorption isotherms were applied. A typical chromatogram obtained by the procedure mentioned in EXPERIMENTAL is shown in Fig.2. It can be seen that the peaks were quite close to Gaussian distribution, so that the Henry constants (K_i) of the 3 components were calculated by the following equation based on the retention volumes ($V_{R,i}$) of the peaks:

$$K_i = \left(\frac{V_{R,i} - V_0}{V_0}\right)\frac{\varepsilon_t}{1-\varepsilon_t},$$

where V_0 is the dead volume of the column.

The adsorption isotherms obtained were as follows:

$$C^*_{p\alpha}=1.72C_{p\alpha}, C^*_{p\gamma}=3.63C_{p\gamma}, C^*_{p\delta}=1.72C_{p\delta}.$$

where subscripts α, γ, and δ denote α-, γ- and δ-tocopherols, respectively.

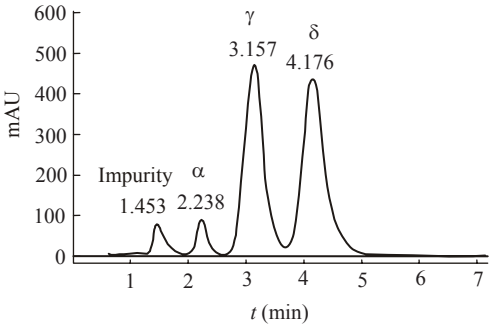

Fig.2 Chromatogram of tocopherols by analytical column. Experimental conditions: silica-gel column (ID 0.46 cm×25 cm); temperature: 30 °C; mobile phase: *n*-hexane: 2-propanol=99:1 (v/v); flow rate: 1.0 ml/min; detector wavelength: 292 nm

Mass-transfer parameters

The mass-transfer parameters required for simulation are intraparticle diffusivity (D_p), axial dispersion coefficient (D_b), and film mass-transfer coefficient (k_f). Approximately effective intraparticle diffusivities were estimated from the Mackie and Meares correlation (Mackie and Meares, 1955):

$$D_p=\left(\frac{\varepsilon_p}{2-\varepsilon_p}\right)\frac{D_m}{\varepsilon_p},$$

where the Brownian diffusion coefficient (D_m) was calculated by the Wilke and Chang correlation (Wilke and Chang, 1955).

The axial dispersion coefficient was estimated by the Chung and Wen correlation (Chung and Wen, 1968), which has been widely used in liquid chromatography.

By using the procedure mentioned in EXPERIMENTAL section, a series of experimental chromatograms were obtained by injections of the tocopherol mixture at different flow rates of the mobile phase. Then the film mass-transfer coefficient (k_f) at different interstitial velocity of mobile phase was obtained by fitting the experimental chromatograms to the general rate model. A typical comparison of experimental chromatogram with the model curves is shown in Fig.3a. The curves coincided with each other quite well.

Results regarding mass-transfer are listed in Table 2. It was found that the relationship between the interstitial velocity u of the mobile phase and the obtained k_f was correlated well with an exponential equation of $k_f=mu^n$.

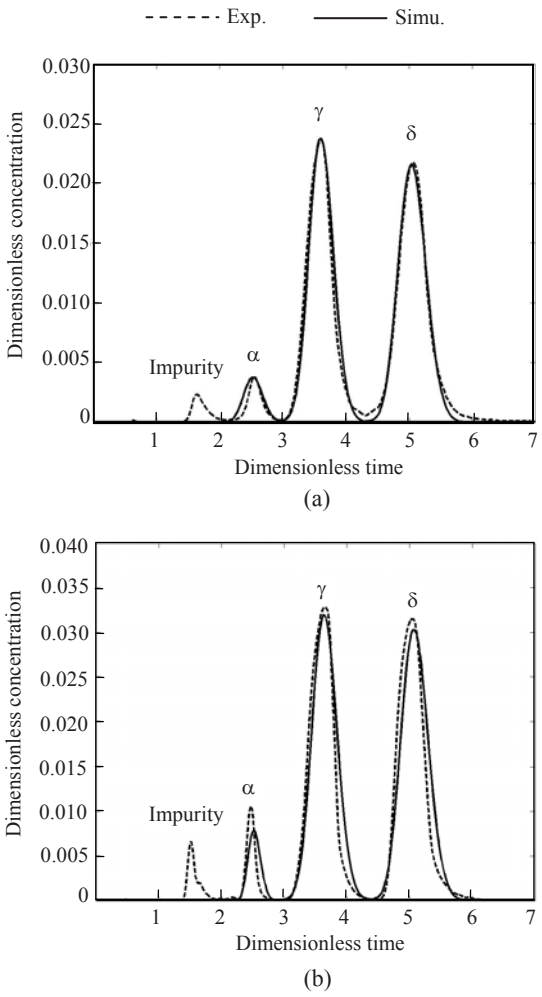

Fig.3 Comparison between experimental results and model simulations for (a) the analytical silica-gel column (ID 0.46 cm×10 cm), under the experimental conditions: column temperature: 30 °C; mobile phase: *n*-hexane:2-propanol (99:1, v/v); flow rate: 0.5 ml/min; injection: 20 μl; detector wavelength: 292 nm; and (b) the preparative silica-gel column (ID 2.0 cm×10 cm), under the experimental conditions: column temperature: 30 °C; mobile phase: *n*-hexane:2-propanol (99:1, v/v); flow rate: 5.0 ml/min; injection: 0.5 ml; detector wavelength: 292 nm

Table 2 Mass-transfer parameters of silica-gel column

Tocopherol	K	D_b (cm^2/s)	k_f (cm/s)*	D_p (cm^2/s)
α-tocopherol	1.72	Chung and Wen (1968)	$k_{f\alpha}=0.171u_\alpha^{0.863}$	2.62×10^{-6}
γ-tocopherol	3.63		$k_{f\gamma}=0.199u_\gamma^{0.898}$	2.67×10^{-6}
δ-tocopherol	5.85		$k_{f\delta}=0.254u_\delta^{0.950}$	2.73×10^{-6}

* Interstitial velocity (u) is between 0.020 and 0.164 cm/s

Scale up from the analytical to SMB columns

The adsorption isotherms and mass-transfer coefficients obtained by the analytical column were used to simulate the chromatographic behavior of an SMB column by the model mentioned above, and thus a simulated chromatogram of the SMB column was obtained. Furthermore, one of the SMB column (No. 1 in Table 1) was used to obtain an experimental chromatogram. Comparison between the simulated and the experimental chromatograms is shown in Fig.3b. The volumetric scale-up factor was about 18.9:1. It can be concluded that the agreement between both the chromatograms was fairly good.

This scale-up method hinges heavily on the assumption that the small column and the large column have the same ε_b and ε_p. This requires that the two columns have the same packing density, which means that the two beds should be operated at similar pressures without one column being much more compressed than the other (Gu, 1995; Gu and Zheng, 1999). Therefore, in this study, the slight difference of bed voidage (0.47 and 0.49) caused the deviation in the scale-up process. Based on the successful simulation of a single SMB column, it can be expected that further simulation of the dynamics and the performance of SMB would be feasible.

Separation of tocopherols by SMB—Simulation and experimental

As it is known that a four-section SMB is usually useful only for the binary separations, therefore the separation of γ-tocopherol and δ-tocopherol is taken as an example here. At first, by using the isotherms and mass-transfer parameters obtained above, the dynamic process of the startup of SMB from the start time to the steady state at a given operating condition was simulated. Then, the composition profile along the columns at steady state was simulated. At last, to evaluate the performance of SMB, the performance parameters of the SMB were calculated according to the simulated results.

Based on the simulation results, experiments were carried out at the same operating conditions as used for the simulation and all the experimental results were compared with those of simulation.

1. Start up of SMB

A typical dynamic process of the startup of SMB, corresponding to the operating condition of run E (Table 3), is shown in Fig.4. Initially, the columns were full of desorbent, and after start of the equipment both average concentrations of δ-tocopherol at the extract port and γ-tocopherol at the raffinate port increased exponentially with switching numbers, finally approaching a cyclic steady state. From the top figures of Figs.4a and 4b, it can be seen that the average concentration of the simulated curves fit to experimental plots quite well. Within each switch, the concentration varied exponentially with time (see the bottom figures of Figs.4a and 4b). Due to the direction of valve switching from columns 1 to 8, the concentration wave was also moving from coulumns 1 to 8. In consequence, at a given port of flow, the concentration of extract decreased with time, while the concentration of raffinate increased with time (refer to Figs.1 and 5). The cyclic steady state was approached after approximately 40 switching times.

2. Composition profile along the columns

After the cyclic steady state was reached the composition profile along the SMB columns at the end of a switching time by run E are presented in Fig.5. It can be seen that the two components are separated in sections 2 and 3 (columns 3 to 6). The concentration of γ-tocopherol decreased with the up stream direction of mobile phase, and at the extract port it became low enough, compared with δ-tocopherol, so that the purity of δ-tocopherol in the extract was ensured. On the other hand, the concentration of δ-tocopherol decreased with the down stream direction of mobile phase. Comparison of the simulated curve with the experimental plots shows that the simulated results are in accordance with the experimental data quite well. Furthermore, at the cyclic steady state, the purity of raffinate and extract predicted by simulation were 98.4% and 99.0%, respectively, very close to the experimental results of 98.3% and 98.9%.

Table 3 Comparison of simulated and experimental performances of SMB

Run	Flow rate (ml/min)					t_s (s)	Purity (%)		Recovery (%)		Desorbent (L/g)		Productivity (g/(h·L))	
	Q_1	Q_2	Q_3	Q_4	Q_F		R	E	R	E	R	E	R	E
A	6.4	4.4	5.1	3.6	0.7	757	99.5	94.2	94.0	99.0	0.363	0.300	1.844	2.232
							99.3	95.0	94.3	99.4	0.346	0.299	1.932	2.238
B	6.4	4.6	5.3	3.6	0.7	757	99.4	98.2	97.6	98.7	0.334	0.301	2.003	2.224
							99.0	98.5	98.3	99.1	0.332	0.300	2.016	2.232
C	6.4	4.9	5.6	3.6	0.7	757	98.4	99.9	99.8	96.9	0.330	0.310	2.047	2.161
							98.8	99.0	98.9	98.9	0.330	0.301	2.027	2.228
D	6.4	5.1	5.8	3.6	0.7	757	95.4	99.9	99.9	95.0	0.326	0.335	2.050	1.999
							98.5	99.4	99.4	98.6	0.328	0.302	2.037	2.221
E	6.4	4.6	5.6	3.6	1.0	757	98.4	99.0	98.7	98.1	0.231	0.212	2.893	3.158
							98.3	98.9	98.8	98.4	0.231	0.211	2.895	3.169
F	6.4	4.4	5.9	3.6	1.5	757	94.9	96.5	95.7	94.4	0.159	0.148	4.209	4.513
							95.7	95.5	95.0	95.9	0.160	0.144	4.178	4.630
G	6.7	4.9	5.9	4.1	1.0	720	98.3	99.2	98.8	99.6	0.214	0.196	2.906	3.169
							98.8	99.3	99.2	98.9	0.314	0.195	2.907	3.183
H	6.9	5.0	6.0	3.8	1.0	708	98.3	99.3	99.8	99.2	0.255	0.230	2.908	3.215
							98.9	99.5	99.0	99.5	0.255	0.230	2.907	3.214

Note: R: raffinate; E: extract; in the columns of performance parameters the data of upper line in each run are simulated results, and the data of lower line are the corresponding experimental results

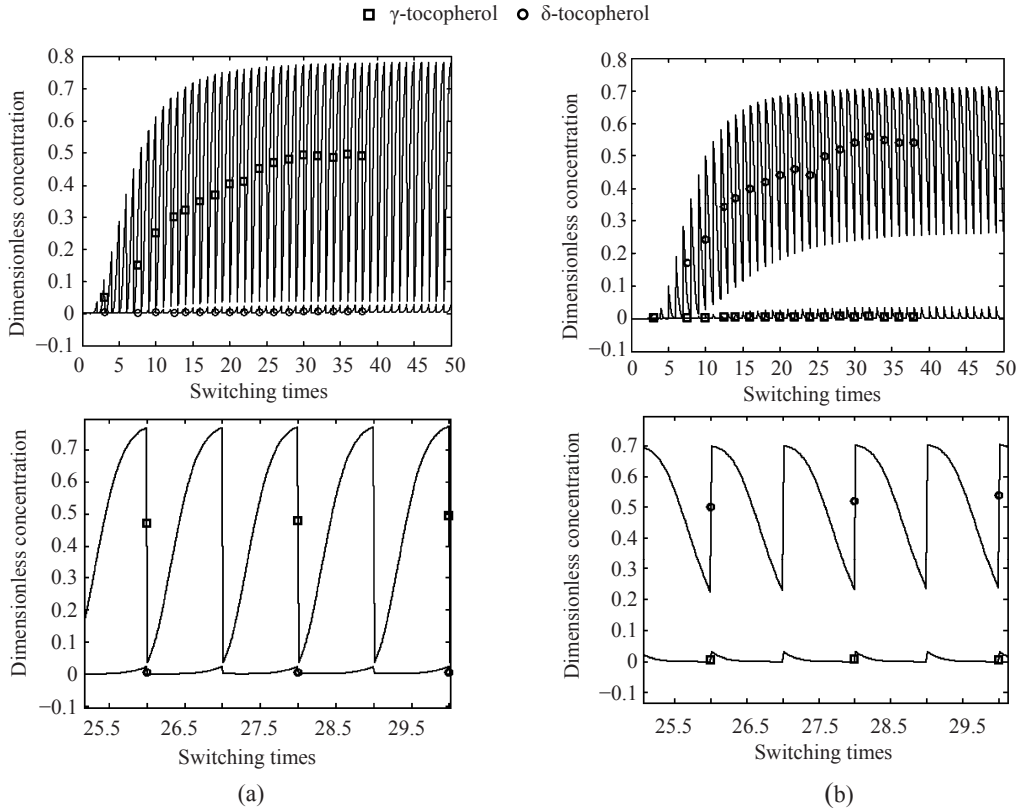

Fig.4 Effluent histories of SMB process (lines are simulation results). (a) Raffinate; (b) Extract

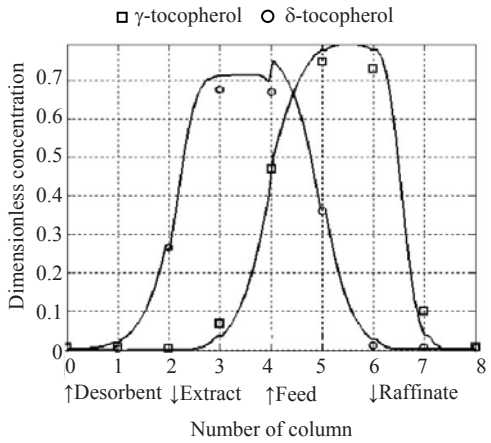

Fig.5 Total column profiles of the four-section SMB. Lines are simulation results

3. Performance of SMB

The main operating conditions affecting the performance of SMB are the flow rate of feed, the flow rate in each section, and switching time. Eight sets of operating conditions were designed to study the effect of the operating condition on the performance of SMB. The SMB performance was evaluated by four process parameters: purity, recovery, productivity and desorbent consumption. The definitions of the parameters are listed in Table 4, where the more retained component *A* was δ-tocopherol, and the less retained component *B* was γ-tocopherol. The experimental results were compared with the simulation (Table 3). Here again, the simulated results of all operating conditions were quite close to the experimental data, indicating that the methodology of the simulation in the present work was reliable.

The effect of the flow rate of feed on the performance parameters is indicated by results of runs C, E and F. As Q_F increased, the productivity increased and the desorbent consumption decreased proportionally. Meanwhile, since the separation ability of the equipment was getting down with Q_F, both the purity and recovery decreased. The decreasing slope was not linear, and the increment of Q_F from runs C to D was the same as that from D to E, but the purity and recovery did not decrease as much from runs C to D as from D to E.

The effects of flow rate in sections 2 and 3 on the purity of extract and raffinate were contradictory. At higher flow rates in these two sections the concentration pattern moved more to the downstream direction of the mobile phase (refer to Fig.5). In consequence, the concentration of γ-tocopherol in extract became less, on the other hand the concentration of δ-tocopherol in raffinate became greater. This fact is shown in the results of runs A to D. As Q_2 and Q_3 increased, the purity of δ-tocopherol in extract increased from 95.0% to 99.4%, while its recovery decreased. However, the purity of γ-tocopherol in raffinate decreased from 99.3% to 98.5%, while its recovery increased.

Rapid switching means that the flow rate of the solid phase relative to the mobile phase is increased. As a result, the separation ability of SMB will increase so that the purity and recovery of both components will increase as well. This effect can be seen from the data of runs E, G and H. As the switching time decreased from 757 to 708 s, the purity of raffinate increased from 98.3% to 98.9% and the purity of extract increased from 98.9% to 99.5%, too. In the meantime the recovery of both components increased as well.

In summary, the simulated results of performance of SMB were quite close to the real process, and the effect of operating conditions on the performance could be studied by simulation. Furthermore, the optimized operating conditions for a given system could be determined by simulation as well. In addition, the separation of α-tocopherol and γ-tocopherol by SMB was studied by the same methodology in this laboratory as a part of the project of separation of all the tocopherol homologues (LÜ, 2006).

Table 4 Definition of the process performance parameters

Performance parameter	Purity (%)	Recovery (%)	Productivity (g/(h·L))	Solvent consumption (L/g)
Extract	$100C_E^A/(C_E^A+C_E^B)$	$100Q_EC_E^A/(Q_FC_F^A)$	$C_E^AQ_E/V_S$	$Q_D/(C_E^AQ_E)$
Raffinate	$100C_R^B/(C_R^A+C_R^B)$	$100Q_RC_R^B/Q_FC_F^B$	$C_R^BQ_R/V_S$	$Q_D/(C_R^BQ_R)$

C_E^A and C_F^A: the concentrations of *A* in extract and feed, respectively; C_R^B and C_F^B: the concentrations of *B* in raffinate and feed, respectively; Q_E, Q_R, Q_D and Q_F: volumetric flow rates of extract, raffinate, desorbent and feed, respectively; V_S: volume of solid phase

CONCLUSION

(1) The simulation of SMB process in the present work is successful. Based on the experimental chromatograms on a single column of analytical size, the dynamics of setup, the composition profile along the columns, and the performance of separation of SMB can be simulated by using the general rate model.

(2) The methodology is valid for optimization of the operating conditions of SMB.

(3) A process for separation and purification of tocopherol homologues by using SMB has been developed successfully. γ-tocopherol and δ-tocopherol with high purity (>98%) and high recovery (>98%) were obtained.

References

Bruce, P., 1998. Simulated moving bed processing: escape from the high-cost box. *Journal of Chromatography A*, **827**(2):143-160. [doi:10.1016/S0021-9673(98)00732-8]

Chung, S.F., Wen, C.Y., 1968. Longitudinal dispersion of liquid flowing through fixed and fluidized beds. *AIChE Journal*, **14**(6):857-866. [doi:10.1002/aic.690140608]

Dunnebier, G., Klatt, K.U., 2000. Modeling and simulation of nonlinear chromatographic separation process: a comparison of different modeling approaches. *Chemical Engineering Science*, **55**(21):373-380. [doi:10.1016/S0009-2509(99)00332-2]

Gu, T., 1995. Mathematical Model and Scale-up of Liquid Chromatography. Springer, Berlin.

Gu, T., Zheng, Y., 1999. A study of the scale-up of reversed-phase liquid chromatography. *Separation and Purification Technology*, **15**(1):41-58. [doi:10.1016/S1383-5866(98)00083-5]

Jupke, A., Epping, A., Schmidt-Traub, H., 2002. Optimal design of batch and simulated moving bed chromatographic separation processes. *Journal of Chromatography A*, **944**(1-2):93-117. [doi:10.1016/S0021-9673(01)01311-5]

LÜ, Y.B., 2006. Study on Separating Natural Products with Simulated Moving Bed. PhD Thesis, Zhejiang University, Hangzhou, China (in Chinese).

LÜ, Y.B., Wei, F., Shen, B., Ren, Q.L., Wu, P.D., 2006. Modeling, simulation of a simulated moving bed for separation of phosphatidylcholine from soybean phospholipids. *Chinese Journal of Chemical Engineering*, **14**(2):171-177. [doi:10.1016/S1004-9541(06)60055-4]

Ma, Z., Wang, N.H.L., 1997. Design of simulated moving bed chromatography using standing wave analysis: linear systems. *AIChE Journal*, **43**(10):2488-2508. [doi:10.1002/aic.690431012]

Mackie, J.S., Meares, P., 1955. The Diffusion of Electrolytes in a Cation Exchange Resin Membrane. Proceedings of the Royal Society of London. Series A, **232**:498-509.

Mazzotti, M., Storti, G., Morbidelli, M., 1997. Optimal operation of simulated moving bed units for nonlinear chromatographic separations. *Journal of Chromatography A*, **769**(1):3-24. [doi:10.1016/S0021-9673(97)00048-4]

Migliorini, C., Mazzotti, M., Morbidelli, M., 1998. Continuous chromatographic separation through simulated moving beds under linear and nonlinear conditions. *Journal of Chromatography A*, **827**(2):161-173. [doi:10.1016/S0021-9673(98)00643-8]

Minceva, M., Rodrigues, A.E., 2002. Modeling and simulation of a simulated moving bed for the separation of *p*-xylene. *Industrial & Engineering Chemistry Research*, **41**(14):3454-3461. [doi:10.1021/ie010095t]

Ruthven, D.M., Ching, C.B., 1989. Counter-current and simulated counter-current adsorption separation process. *Chemical Engineering Science*, **44**(5):1011-1038. [doi:10.1016/0009-2509(89)87002-2]

Schulte, M., Strube, J., 2001. Preparative enantioseparation by simulated moving bed chromatography. *Journal of Chromatography A*, **906**(1-2):399-416. [doi:10.1016/S0021-9673(00)00956-0]

Wilke, C.R., Chang, P.C., 1955. Correlations of diffusion coefficients in dilute solutions. *AIChE Journal*, **1**(2):264. [doi:10.1002/aic.690010222]

Xie, Y., Hritzko, B., Chin, C.Y., Wang, N.H.L., 2003. Separation of FTC-ester enantiomers using a simulated moving bed. *Industrial & Engineering Chemistry Research*, **42**(17):4055-4067. [doi:10.1021/ie030225t]

Yang, Y.W., Wen, G.D., Wu, C.J., Ren, Q.L., Wu, P.D., 2004. Preparation of natural α-tocopherol from non-α-tocopherols. *Journal of Zhejiang University SCIENCE*, **5**(12):1524-1527. [doi:10.1631/jzus.2004.1524]

Zhong, G.M., Guiochon, G., 1998. Steady-state analysis of simulated moving bed chromatography using the linear, ideal model. *Chemical Engineering Science*, **53**(6):1121-1130. [doi:10.1016/S0009-2509(97)00401-6]